

Atomic Josephson vortex

V.M. Kaurov and A.B. Kuklov

*Department of Engineering Science and Physics,
The College of Staten Island, CUNY, Staten Island, New York 10314*

(Dated: November 18, 2018)

We show that Josephson vortices in a quasi-1D atomic Bose Josephson junction can be controllably manipulated by imposing a difference of chemical potentials on the atomic BEC waveguides forming the junction. This effect, which has its origin in the Berry phase structure of a vortex, turns out to be very robust in the whole range of the parameters where such vortices can exist. We also propose that a Josephson vortex can be created by the phase imprinting technique and can be identified by a specific *tangential* feature in the interference picture produced by expanding clouds released from the waveguides.

PACS numbers: 03.75.Lm, 03.75.Kk, 11.30.Qc

I. INTRODUCTION

From the very beginning of the experimental achievement of Bose-Einstein condensation in trapped ultracold gases, various solitonic and topological collective structures, such as dark [1] and bright [2] solitons, vortices [3], skyrmions [4], etc., became objects of great theoretical and experimental interest. These configurations are direct manifestations of macroscopic coherence of BEC and many of them were repeatedly created and detected.

In our previous work [5] it has been shown that yet another stable object, namely atomic Bose Josephson vortex (JV), can exist in a long Bose Josephson junction (BJJ). Such junction can be formed between two parallel quasi-1D Bose Einstein condensates coupled by tunneling. The circulating atomic supercurrents — counter-propagating in each waveguide and closing the loop between them — represent a neutral analog of the Josephson vortex studied in superconducting Josephson junctions in great detail [8]. While bearing similarities with the charged case, the absence of the Meissner effect makes the local formulation of the BJJ solution possible only in a quasi-1D geometry. The most interesting feature of the Bose JV is its interconversion into a dark soliton (DS) [5]. Accordingly, the description of the Bose JV necessarily involves both the phase and the amplitude of the wavefunction. This instability, which can be controlled by tuning the Josephson coupling, may potentially be utilized in several ways [5]. Here we show that the Berry phase term is responsible for a force produced on the JV by a time-dependent difference of the chemical potentials $\delta\mu$ applied between the waveguides. Once the JV speed as a whole reaches a certain critical value, the instability destroying the supercurrent circulation develops so that the JV transforms into a moving DS (grey soliton) which is essentially insensitive to $\delta\mu$. We also discuss how the phase imprinting method and the interference after some free expansion can be employed for creating and detecting the JV. As it turns out, the formation of the relative phase between the waveguides is quite insensitive to the characteristics of the imprinting beams once certain topological requirements are satisfied. The JV introduces a

specific *tangential* feature into the interference pattern, which should allow an unambiguous identification of the JV as well as of the interconversion effect [5].

Experimental tools with great potential for creation, manipulation and detection of the JV have already become available and continue to develop. Long BJJ consisting of two parallel coupled atomic waveguides was experimentally realized with two different and equally versatile techniques capable of producing double-well potential of necessary geometry. First technique uses counter-propagating laser beams to form an optical dipole trap [6] and second one uses a microfabricated atom chip with purely magnetic potential [7]. In both cases relative coherence of BECs has been revealed in the interference fringes.

II. ATOMIC QUASI-1D JOSEPHSON VORTEX

Below we will introduce a phenomenological description of the atomic JV which captures three main effects: i) The JV instability with respect to its interconversion into the DS as the Josephson coupling strength exceeds certain threshold [5]; ii) The critical speed effect; iii) The effect of force on the JV produced by uniform $\delta\mu$. We will also derive the corresponding phenomenological coefficients in terms of the microscopic model [5] close to the threshold and will consider the opposite limit — very small couplings, when the JV can be well described by the Sine-Gordon (SG) equation.

A. Phenomenological free energy

Phenomenological description helps elucidating generic features which do not depend qualitatively on a particular microscopic model. The main characteristic of the JV is a presence of a localized supercurrent circulation degenerate with respect to its orientation. This circulation can be described by persistent currents $J_{1,2}(x, t)$ along the first and the second waveguides, respectively, as well as by tunneling Josephson currents between the wave-

uities. Here x is a spatial coordinate along two parallel waveguides and t stands for time. If the JV is stationary, the currents $J_{1,2}(x, t)$ are localized within some typical distance and flow in opposite directions, and, therefore, the difference $J(t) = \int dx(J_1(x, t) - J_2(x, t))$ is a good global measure of the circulation. Obviously, the quantity $P(t) = \int dx(J_1(x, t) + J_2(x, t))$ is linear momentum of the JV. It is zero, if the JV is stationary, and it must acquire a finite value, if it is moving as a whole. The total momentum is assigned to center of mass of the JV positioned somewhere at $X_0(t)$ along the junction. This generic picture is well known from the phenomenological description of the JV in superconductors [8], where the SG model is sufficient to find the relation between $P(t)$ and the center of mass velocity $V = \dot{X}_0$ through the JV effective mass M .

It is important that in the SG model the circulation is essentially a topologically conserved quantity (provided the contribution to the circulation from the tunneling currents are negligible). Thus, this model does not contain the interconversion effect [5] taking place in a quasi-1D geometry. Incorporating density fluctuations shows that the center of mass position X_0 can be associated with a dip in the condensate densities in each waveguide. This dip becomes more pronounced as the Josephson coupling γ strengthens, and, finally, it becomes zero of the densities at some critical value $\gamma = \gamma_c$, which signals a moment of the transformation of the JV into the DS. At this point and for higher γ no more current circulation J exists. Obviously, this effect can be interpreted in terms of spontaneous breaking of time reversal symmetry for $\gamma < \gamma_c$ with the order parameter $J \neq 0$. Since J is just one degree of freedom the corresponding "phase transition" occurs in zero spatial dimensions and therefore cannot be considered as a true phase transition. Yet, the corresponding free energy of the system containing just one DS or JV can be represented in a sense of the Landau expansion of the effective action close to the "critical" point $\gamma \approx \gamma_c$ as

$$\mathcal{L}_{eff} = \dot{X}_0 P + \dot{Q} J - \mathcal{H}_{eff}, \quad (1)$$

with the effective Hamiltonian being

$$\mathcal{H} = \frac{P^2}{2M_+} + \frac{Q^2}{2M_-} + \alpha(\gamma - \gamma_c) J^2 + c_1 J^4 - c_2 \delta\mu P J + c_3 J^2 P^2. \quad (2)$$

where $Q(t)$ stands for a variable canonically conjugate J ; M_+ , M_- , $\alpha > 0$, $c_1 > 0$, $c_2, c_3 > 0$ are phenomenological coefficients dependent on a particular form of a microscopic description. These coefficients will be determined later within the variational approach applied to the model [5].

The Lagrangian (1,2) describes the effect i), that is, spontaneous formation of the circulation $J \neq 0$ for $\gamma < \gamma_c$ [5] ($c_1 > 0$ insures stability beyond linear approximation) as well as coupling between the center of mass motion and the internal circulation.

The term $\sim c_3$ accounts for the effect ii): as $P \sim V$ exceeds some critical value, the effective coefficient $\alpha(\gamma -$

$\gamma_c) + c_3 P^2$ becomes positive, which restores the time-reversal symmetry so that the circulation $J = 0$.

The term $\sim c_2$ is responsible for the effect iii), that is, for the force induced by $\delta\mu$. This term is symmetric with respect to exchanging of the waveguides and conforms with the time-reversal symmetry. Indeed, swapping the waveguides positions changes $\delta\mu \rightarrow -\delta\mu$ and $J \rightarrow -J$. The time-reversal leaves the product $J P$ invariant. The term $\delta\mu P J$ is responsible for the force $\sim \delta\mu J$ on the JV. Its origin can be understood as follows: When $\delta\mu \neq 0$, a number of atoms $\sim \delta\mu$ starts tunneling between the waveguides. Accordingly, the first and the second waveguides acquire the total linear momenta $\sim \delta\mu \int dx J_1$ and $\sim -\delta\mu \int dx J_2$, respectively. Hence, the total momentum P attains a nonzero value $\sim \delta\mu J$ as long as the circulation J is finite. The force, then, is $\dot{P} \sim \delta\mu J$. It can also be viewed as a force due to the bias introduced by the tunneling currents driven by $\delta\mu$ (compare with the bias term in the SG equation [8]).

In the presence of dissipation one should introduce the dissipative function in terms of the velocities \dot{X}_0 and \dot{Q} as

$$\mathcal{F} = \frac{\dot{X}_0^2}{2\sigma_+} + \frac{\dot{Q}^2}{2\sigma_-}, \quad (3)$$

with some kinetic coefficients $\sigma_{\pm} > 0$. Then the standard variational procedure with respect to the conjugate variables yields the equations of motion

$$V - \left(\frac{1}{M_+} + 2c_3 J^2 \right) P - c_2 \delta\mu J = 0, \quad (4)$$

$$\dot{P} + \frac{V}{\sigma_+} = 0, \quad (5)$$

$$\dot{Q} - 2(\alpha(\gamma - \gamma_c) + c_3 P^2) J - 4c_1 J^3 - c_2 \delta\mu P = 0, \quad (6)$$

$$\dot{J} + \frac{Q}{M_-} + \frac{\dot{Q}}{\sigma_-} = 0. \quad (7)$$

This system describes a quite complex non-linear dynamics of the circulation J coupled to the center of mass motion. Besides small oscillations of J around equilibrium, strongly non-linear evolution of J corresponding to the phase-slip, during which J changes sign, can occur as γ approaches γ_c from below. The term $\sim c_3$ in eq.(6) is responsible for strong coupling of the phase-slip to the motion of the JV as a whole. Furthermore, the terms $\sim \delta\mu$ introduces the parametrical driving. Thus, all three effects mentioned above cannot in general be well separated from each other, and general solution of the system can only be obtained numerically. However, considering certain limiting cases is helpful for making these effects independent from each other. So, in what follows we will consider such limiting situations. In reality, of course, the above system should be analyzed numerically.

Let us, first, consider the case $\delta\mu = 0$ and $P = 0$, that is, stationary JV. Then, eqs.(6,7) are essentially those discussed in ref.[5] which describe the dynamics

of the JV-DS interconversion which involves the phase-slip. Here we will not discuss this effect (that is, i)) any further.

The effect ii) makes sense to consider only in the case of small dissipation with respect the center of mass motion. So, we set $1/\sigma_+ = 0$ and, keeping $\delta\mu = 0$, find that the generalized momentum is conserved $P = \text{const}$. Then, eq.(4) gives $P = M_+V$ in the limit of small J . Further substitution into eq.(6) yields $-2(\alpha(\gamma - \gamma_c) + c_3M_+^2V^2)J - 4c_1J^3 = 0$ in equilibrium. A non-trivial solution exists only when the coefficient $\alpha(\gamma - \gamma_c) + c_3M_+^2V^2$ in front the linear term in eq.(6) is negative. Accordingly, the critical velocity becomes

$$V_c = V_1\sqrt{\gamma_c - \gamma}, \quad V_1 = \sqrt{\frac{\alpha}{c_3M_+^2}}, \quad (8)$$

above which no quasi-static solution for the circulation $J \neq 0$ exists.

Now, let's consider the effect iii) where $\delta\mu \neq 0$ and small. Then, we assume that velocities are much smaller than the critical one (8) and the JV circulation parameter J is in equilibrium close to its value $J_0 = \pm\sqrt{\alpha(\gamma_c - \gamma)}/2c_1$ determined when $V = 0$. In this situation, one should ignore the term $\sim c_2$ in eq.(6) because it describes just a small correction to J_0 . Subsequently, J can be replaced by J_0 in eq.(4) and term $\sim c_3$ should be dropped because it describes a small correction $\sim \gamma_c - \gamma$ to the finite term $1/M_+$. Then, excluding P , one finds that the center of mass velocity obeys the equation

$$\dot{V} + \frac{V}{M_+\sigma_+} = \frac{f(t)}{M_+}, \quad f(t) = c_2M_+J\delta\mu. \quad (9)$$

As discussed above, the term $f(t)$ describes the force induced by time dependence of the difference of the chemical potentials $\delta\mu$. The relation of this force to the Berry phase term in the full "microscopic" action will be considered below.

B. Variational approach

It is worth noting that all the phenomenological coefficients can be derived from a "microscopic" Lagrangian and a dissipative function. Here we will use a simplified approach which ignores dissipation and will consider model [5] as the "microscopic" Lagrangian. In terms of the fields $\psi_{1,2}$ describing each waveguide the Lagrangian,

$$\mathcal{L} = \mathcal{L}_B - \mathcal{H}, \quad (10)$$

is given by the Berry term

$$\mathcal{L}_B = \text{Re} \int dx \left[i\hbar(\psi_1^*\dot{\psi}_1 + \psi_2^*\dot{\psi}_2) \right], \quad (11)$$

and by the Hamiltonian

$$\mathcal{H} = \mathcal{H}_1 + \mathcal{H}_2 + \mathcal{H}_{12}, \quad (12)$$

consisting of the each waveguide terms

$$\mathcal{H}_k = \int dx \left[\frac{\hbar^2}{2m} |\nabla\psi_k|^2 + \frac{g}{2} |\psi_k|^4 - \mu_k |\psi_k|^2 \right], \quad (13)$$

with $k = 1, 2$, and of the contribution which describes the Josephson tunneling between the waveguides

$$\mathcal{H}_{12} = - \int dx \gamma (\psi_1^*\psi_2 + \psi_2^*\psi_1), \quad (14)$$

where μ_k are waveguide's chemical potentials and the integration $\int dx \dots$ is performed along the waveguides.

The equations of motion following from eqs.(10-14) in the units $\hbar = 1, m = 1$, with the unit of length given by the healing length $l_c = 1/\sqrt{\mu}$ for $\mu = (\mu_1 + \mu_2)/2$ and the unit of time determined by $t_0 = 1/\mu$, are

$$i\dot{\psi}_1 = -\frac{\nabla^2}{2}\psi_1 - (1 + \eta)\psi_1 + |\psi_1|^2\psi_1 - \nu\psi_2; \quad (15)$$

$$i\dot{\psi}_2 = -\frac{\nabla^2}{2}\psi_2 - (1 - \eta)\psi_2 + |\psi_2|^2\psi_2 - \nu\psi_1. \quad (16)$$

Here the wave functions were transformed as $\psi_k \rightarrow \sqrt{n_0}\psi_k$, where $n_0 = \mu/g$ is the average 1D density of a single uncoupled ($\gamma = 0$) waveguide; the quantity ν represents the dimensionless Josephson coupling $\nu = \gamma/\mu$, and η stands for the difference of chemical potentials rescaled by 2μ . These equations admit exact JV stationary solution discussed in detail in ref.[5]. For small velocity of the JV, it is natural to use the variational ansatz which coincides with the stationary solution at $V = 0$. Thus, we choose

$$\Psi_{1,2} = \sqrt{n_{1,2}} \text{th}(s(x - X_0(t))) + \frac{i\sqrt{s}Q_{1,2}}{\text{ch}(s(x - X_0(t)))} \quad (17)$$

with the parameter s giving the JV size. The bulk densities $n_{1,2}$ can be obtained in the thermodynamical limit (when no JV is present) from eqs.(15,16). Since we are interested in small deviations only, the corresponding explicit expressions are

$$n_{1,2} = (1 + \nu) \left(1 \pm \frac{\eta}{1 + 2\nu} + o(\eta^2) \right), \quad (18)$$

where the indexes 1, 2 correspond to \pm , respectively.

The stationary solution [5] can be obtained from the ansatz (17) by setting $X_0 = \text{const}$, $\sqrt{s}Q_1 = -\sqrt{s}Q_2 = \pm\sqrt{1 - 3\nu}$ and $s = 2\sqrt{\nu}$ (compare with ref.[5]). Considering complex $Q_{1,2}$ and real X_0 as slow dynamical variables, one can substitute the ansatz (17) into the Lagrangian (10-14) and perform explicit integration over x . This procedure generates the effective Lagrangian \mathcal{L}_e in terms of the variables $Q_{1,2}$, X_0 , s and their time-derivatives. Obviously, such procedure is in line with separation of fast and slow variables, so that only slow dynamics should be considered to full extent. Close to the interconversion instability ($\nu \approx \nu_c = \gamma_c/\mu$), the slow variables are X_0 and J . The variable s describes fast

adjustment of the JV size. It is important that it is not dynamical within the chosen ansatz. Indeed, as can be seen, the effective Lagrangian does not contain \dot{s} . The choice of s is dictated by conservation of total number of particles during dynamical evolution of the other parameters. Calculating the depletion δN of the number of particles caused by the presence of the JV, we find

$$\delta N = -\frac{2(n_1 + n_2)}{s} + 2(|Q_1|^2 + |Q_2|^2) = C_N, \quad (19)$$

where the constant C_N is determined for the stationary JV by setting all the time derivatives to zero and minimizing the effective energy with respect to $Q_{1,2}$ and s . Considering small values η , it is enough to set $n_1 + n_2 = 2(1 + \nu)$, which is the equilibrium value. Here we will consider values $Q_{1,2} \rightarrow 0$, so that the explicit solution of eq.(19) for s becomes

$$s = \sqrt{1 + \nu} + \frac{1 - 3\nu}{2\sqrt{1 + \nu}} - \frac{|Q_1|^2 + |Q_2|^2}{2}. \quad (20)$$

As discussed in ref.[5], the value $\nu = \nu_c = 1/3$ is the critical point below which the JV forms spontaneously from the DS. Thus, the smallness of $Q_{1,2}$ automatically implies a proximity to the critical point. Then, for consistency of the effective action expressed in powers of $Q_{1,2}$, the value ν should be set to ν_c except in the quadratic term vanishing at the critical point.

It is worth discussing, first, the structure of the Berry-term part (11) of the full action. As mentioned above, the cross term $\sim \eta P J$ leading to the force on the JV $\sim \dot{\eta}$ in the Lagrangian (1) can be viewed as generated by the Berry phase effect. Indeed, the Berry part is $\mathcal{L}_B = \int dx(-\rho_1 \dot{\varphi}_1 - \rho_2 \dot{\varphi}_2)$, where ρ_k and φ_k are density and the phase, respectively, in the k -th waveguide. In the static solution [5] as well as in the ansatz (17) each phase changes by $\pm\pi$, so that, e.g., if at $x = -\infty$ one finds $\varphi_1 = \varphi_2 = 0$, then, at $x = +\infty$ there is $\varphi_1 - \varphi_2 = 2\pi$. If the JV is moving slowly, then $\dot{\varphi}_k \approx \dot{X}_0 \nabla \varphi_k$. Thus, a substitution into the Berry part gives $\mathcal{L}_B \approx \dot{X}_0 \int dx(\rho_1 \nabla \varphi_1 + \rho_2 \nabla \varphi_2) \approx \pi \dot{X}_0(\rho_1 - \rho_2)$, where spatial variations of the densities are ignored. Flipping the time derivative and realizing that $\rho_1 - \rho_2 \sim \eta$, one finds $\mathcal{L}_B \sim -X_0 \dot{\eta}$, which is the work done while making a displacement X_0 by the force $\sim \dot{\eta}$.

The relation between the observables P, J can be obtained as a result of substituting the ansatz (17) into (11). This yields $\mathcal{L}_B = \dot{X}_0 P - 2(\dot{B}_+ Q_+ + \dot{B}_- Q_-)$, where $Q_+ = \text{Re}(Q_1 + Q_2)$, $Q_- = \text{Re}(Q_1 - Q_2)$, $B_+ = \text{Im}(Q_1 + Q_2)$ and $B_- = \text{Im}(Q_1 - Q_2)$. The total momentum $P = -i \int dx(\psi_1^* \nabla \psi_1 + \psi_2^* \nabla \psi_2)$ and the supercurrent circulation $J = -i \int dx(\psi_1^* \nabla \psi_1 - \psi_2^* \nabla \psi_2)$ are given as

$$P = -\pi(1 + \nu)^{3/4} \left[Q_+ + \frac{\eta Q_-}{2(1 + 2\nu)} \right], \quad (21)$$

$$J = -\pi(1 + \nu)^{3/4} \left[Q_- + \frac{\eta Q_+}{2(1 + 2\nu)} \right]. \quad (22)$$

Thus, the parameters Q_{\pm} can uniquely be expressed in terms of P, J . In particular, $Q_+ \sim P$ for $\eta = 0$. The Berry phase effect discussed above is reflected in the part $\sim \eta$ of eq.(21). It is also clear that the variable conjugated to J in eq.(1) is $Q \sim B_-$. Further analysis shows that the quantity $B_+ = \text{Im}(Q_1 + Q_2)$ enters \mathcal{L}_B in a combination $\sim \dot{B}_+ P - r_b B_+^2 + o(B_+^4)$ with some $r_b > 0$. Thus, B_+ would generate higher time derivatives with respect to X_0 , which should be neglected as long as the JV motion is slow. Accordingly, it is reasonable to set $B_+ = 0$ in eq.(17), so that $Q_{1,2}$ are chosen in the form

$$Q_{1,2} = \frac{Q_+ \pm Q_-}{2} \pm i \frac{B_-}{2}, \quad (23)$$

with the indexes 1, 2 corresponding to \pm , respectively. Finally, employing the ansatz (17,23) in the "microscopic" Lagrangian (10-14) and expressing the variables (23) in terms of the observables P, X_0, Q, J as described above one arrives at the effective Lagrangian in the form (1), where the coefficients (in the chosen units) are

$$\frac{1}{M_+} = -\frac{\sqrt{3}}{2\pi^2}, \quad (24)$$

$$\frac{1}{M_-} = \frac{32\pi^2}{27\sqrt{3}}, \quad (25)$$

$$\alpha(\gamma - \gamma_c) = \frac{3\sqrt{3}}{4\pi^2} \left(\nu - \frac{1}{3} \right), \quad (26)$$

$$c_1 = \frac{3\sqrt{3}}{128\pi^4}, \quad (27)$$

$$c_2 = \frac{2\sqrt{3}}{5\pi^2}, \quad (28)$$

$$c_3 = \frac{9\sqrt{3}}{64\pi^4}. \quad (29)$$

In these expressions, the difference $\sim \nu - \nu_c$ has been ignored except in the quadratic coefficient (26), which determines the instability.

It is worth noting that far from the instability (that is, $\nu \ll \nu_c$) no simple expansion for the effective Lagrangian in terms of powers of $Q_{1,2}$ can be obtained. However, it is clear that in this limit, the variations of the density can be ignored as long as the JV is close to its internal equilibrium. Thus, the effective action can simply be obtained by considering fluctuations of the densities being small. This will lead to the SG model. For completeness, we will consider this limit below.

C. Sine-Gordon approximation

Setting $\psi_1 = \sqrt{n_1 + n'_1(x, t)} \exp(i\varphi)$, $\psi_2 = \sqrt{n_2 + n'_2(x, t)} \exp(i\varphi)$, with $n_{1,2}$ being uniform background densities given by eq.(18) and $n'_{1,2}$ describing small fluctuations, and substituting this into the action (10) one obtains the effective Lagrangian in terms of the

relative phase φ only as

$$\mathcal{L}_{SG} = \int dx [(n_2 - n_1)\dot{\varphi} + \dot{\varphi}^2 - (1 + \nu)(\nabla\varphi)^2 + 2\nu(1 + \nu)\cos(2\varphi)], \quad (30)$$

where $n'_{1,2}$ were eliminated in the long wave limit, with the gradients of $n'_{1,2}$ ignored; the difference $n_2 - n_1 \neq 0$ has only been retained in the Berry term.

The variation yields

$$\ddot{\varphi} - (1 + \nu)\nabla^2\varphi + 4\nu(1 + \nu)\sin(2\varphi) = \dot{n}_1 - \dot{n}_2 \quad (31)$$

the biased SG equation with its well known solution in the static limit (see in [8]). It is important to note that this equation exhibits Lorentz invariance (for $\dot{n}_1 - \dot{n}_2 = 0$). Hence, no the critical velocity effect ii) can be described in the SG approximation.

Here we will be interested the limit of slow velocity V and small $\dot{n}_1 - \dot{n}_2$ in eq.(31). Then, one can use the static SG solution, with its center of mass velocity V being a slow variable [8], in the Lagrangian (30). Then, integrating explicitly, one finds

$$\mathcal{L}_{SG} = \int dx [-2\pi\eta V + \frac{M_{SG}V^2}{2}] \quad (32)$$

where the effective mass is

$$M_{SG} = 4\sqrt{2\nu}. \quad (33)$$

Varying with respect to X_0 and including the dissipative function, one arrives at the equation similar to eq.(9):

$$\dot{V} + \frac{V}{\sigma_+ M_{SG}} = \frac{2\pi\dot{\eta}}{M_{SG}}, \quad (34)$$

which describes the effect of force induced by the Berry term. Thus, while a particular expression for the force depends on the proximity to ν_c , the effect persists for all values $\nu < \nu_c$.

D. Numerical simulation of the Berry phase effect

Sensitivity to the difference of the chemical potentials η can be a useful tool for manipulation of the JV position in the junction. To demonstrate this numerically we used η as an externally controlled variable to displace the JV on a distance much greater than its size and, then, to return it to its original position. The result of the simulations of the full system (15, 16) is displayed on FIG.1. The plot on the left represents density of a single waveguide by the intensity of white color. The dark curve is a trajectory of the JV center, where its density is minimal. Shown on the right, the time-dependence η is chosen as $\eta(t) = 0.1 \sin(\omega t)$, with $\omega = \pi/125$. The simulations have been performed with the dissipative term introduced in ref.[5]. It is important to note that the

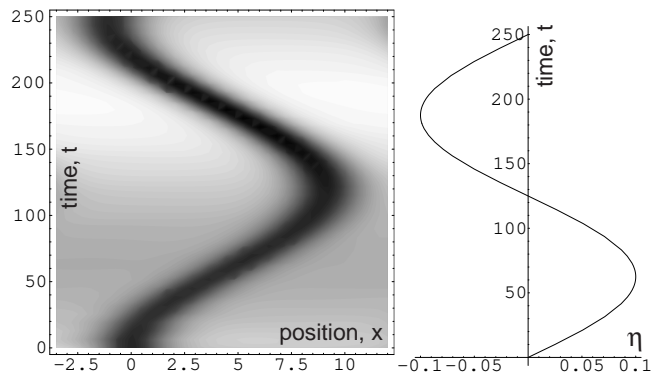


FIG. 1: Motion of the JV along the junction (left) generated by change of relative chemical potential η (right) from numerical simulations of the system (15, 16). Left figure: the atomic density in a single waveguide is represented by intensity of white color; the JV path in x - t coordinates corresponds to the dark color (the density depletion in the JV center) relative to the white color of the background. Here $\nu = 0.1$, and the dissipative term from ref.[5] is given by the value of the kinetic parameter $\tilde{\sigma} = 2$. The units of x and t are the coherence length l_c and the coherence time t_0 , respectively.

regime chosen for numerical simulations is neither close to the critical point nor to the SG limit. Yet, the time dependence $X_0(t) = A(1 - \cos(\omega t))$, which follows from eqs.(9,34) in the limit of small damping and where A is some amplitude, is consistent with the simulations with the reservation that the numerical value of A is not reproduced correctly by either limiting approximation: while eq.(9) underestimates A by a factor of 2, the SG limit (34) overestimates it by a factor of 4.

III. CREATION BY PHASE IMPRINTING

The JV can be formed as a result of the decay of the DS, once the Josephson coupling γ is reduced below a critical value γ_c (or, in the chosen units, ν , with the critical value being $\nu_c = 1/3$) [5]. An alternative method is the phase imprinting. It is already a well established experimental tool for creation of the DS [1]. It consists of exposing a BEC to a pulse of a far detuned laser beam which acts as a temporary external potential $U(x, t)$. According to the impulse approximation, the duration of the pulse δt must be short compared to the correlation time of the condensate $t_0 = 1/\mu$, so that no change of the BEC density occurs during the pulse — atoms just acquire finite speeds without performing any significant displacements. The phase, on the other hand, accumulates according to $\delta\varphi(x) = \int dt U(x, t)$ and the wave function ψ before the pulse is transformed as $\psi \rightarrow e^{-i\delta\varphi}\psi$ after the pulse. To create a DS, one needs to expose a half-plane of an elongated BEC to a laser pulse with a spatial variation reminiscent of the typical DS phase profile (the

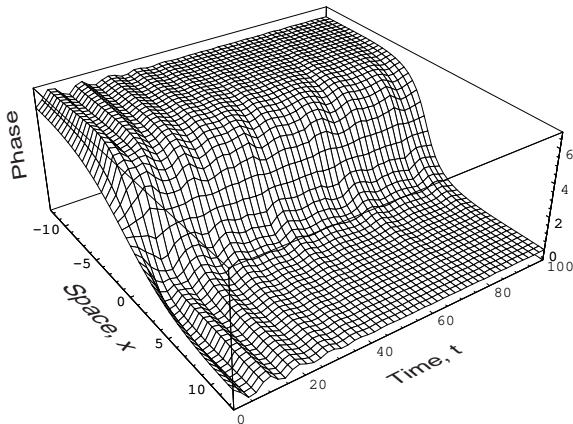


FIG. 2: Evolution of the relative phase after the imprinting as follows from eqs.(15,16). Small dissipative term discussed in ref.[5] with $\tilde{\sigma} = 6$ has been added; $\nu = 0.1$. The units of x and t are the coherence length l_c and the coherence time t_0 respectively.

π -step). In order to produce the JV, one needs to apply a pulse with spatial profiles $U_{1,2}(x, t)$ specific for each waveguide. These should reflect the structure of the JV phases in each waveguide: $\varphi_{1,2} = 0$ at ,e.g., $x = -\infty$ and $\varphi_1 = -\varphi_2 = \pm\pi$ at $x = +\infty$, with smooth transition in between at a typical length comparable to the JV size $= 1/(2\sqrt{\nu})$. Accordingly, $U_{1,2}(x, t) = 0$ at $x = -\infty$ and $U_1(x, t) = -U_2(x, t)$ at $x = +\infty$, with the "crossover" region being approximately equal to the JV size and the time integral $\int dt U_1(x, t) = \pi$ at $x \rightarrow +\infty$.

It is important to note that, once the above "topological" requirements are satisfied, the JV forms with minimal disturbances regardless of other details of the laser beams profiles. The most robust characteristic of the evolving solution turns out to be the phase difference between the waveguides. In the case of the DS, the complete density depletion must form at the DS center. Thus, the adjustment is accompanied by a strong perturbation in the form of the density waves [1]. The depletion at the JV center is also strong, if ν is close to the critical value $1/3$. Accordingly, the densities in each waveguide will experience significant perturbations. Yet, the phase difference relaxes quite smoothly to the equilibrium profile. To demonstrate this feature, we ran numerical simulations with the initially imprinted profile of the phases given by the tanh-type variations of the light intensities as described above. The result of the following evolution of the phase difference is represented on FIG.2. As can be seen, the equilibrium phase profile establishes after few relatively small oscillations even though the initial extension of the (imprinted) phase was about two times longer than the equilibrium JV size.

IV. DETECTION BY INTERFERENCE

Experimental visualization is typically done by absorption imaging [6, 9, 10], with its intensity proportional to the density n of the expanding cloud. In contrast to bulk vortices, which can be detected by observing their cores, the JV does not have a core. Yet, the phases exhibit the π -jumps. Thus, the interference of the expanding clouds released from the waveguides should demonstrate a corresponding feature.

In quasi-1D regime a good approximation for the waveguides wave functions in transverse directions is the Gaussians $G(y, z) = \exp(-(y^2 + z^2)/2d^2)$, with d being a typical width of each waveguide. Thus, in 3D, the two waveguides separated by a distance $2z_0$ can be described by the following ansatz:

$$\Psi_0(\vec{R}) = \Psi_0^+ + \Psi_0^- \quad (35)$$

$$\Psi_0^\pm = f(x)\psi_{1,2}(x)G(y, z \pm z_0) \quad (36)$$

where $\psi_{1,2}(x)$ are the solutions (17) corresponding to either the DS ($Q_{1,2} = 0$) or to the JV and the sign \pm is different for different waveguides. The envelope $f(x) = (1 - (4x^2/L))$, with L , the axial system size, being much larger than the JV, reflects finiteness of the BEC clouds.

As long as the transverse dimension d is much smaller than any axial feature, the expansion occurs primarily in the transverse direction. Thus, the density decreases, practically instantaneously, so that the expansion is essentially free of interaction. This can be formulated as the requirement $(d/l_c)^2 \ll 1$. Indeed, the mean-field interaction is given by the chemical potential $\mu \sim n(t)$, where $n(t) \sim 1/R^2(t)$ stands for a typical density of the expanding cloud scaled by its radius $R(t) \approx \sqrt{d^2 + (t/d)^2}$ (in chosen units). The interaction-induced additional phase shift can be estimated as $\Delta\phi \approx \int_0^\infty \mu dt \sim \int_0^\infty n dt \approx (d/l_c)^2 \ll 1$, where the initial density is taken as $n = 1$ in the chosen units. Hence, under this condition, the density after time t of free expansion becomes

$$n(\vec{R}, t) = \frac{1}{t^3} \left| \int d^3 R' \exp\left(\frac{i(\vec{R} - \vec{R}')^2}{2t}\right) \Psi_0(\vec{R}') \right|^2. \quad (37)$$

A numerical factor in (37) is set to 1, because it defines only overall intensity (not the structure) of the absorption image.

When two expanding uniform BECs overlap they form an interference pattern (IP) of parallel fringes [6, 9]. The specific signature of a rotational vortex in the IP is a so-called edge dislocation. It was predicted in ref.[11] and then seen experimentally in ref.[10]. Here we will discuss how the JV can be recognized in the IP.

For any feature with a size $\sim L_s$ comparable with the healing length to become optically resolvable it must be enlarged (typically about 10 times) during the expansion. We consider the situation when axial expansion of

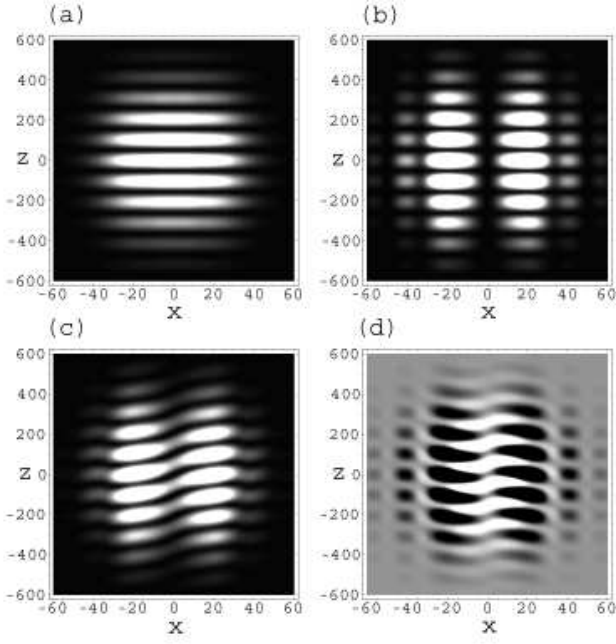


FIG. 3: Interference patterns of two expanded overlapping BEC clouds released from the waveguides as given by direct numerical integration of (37). Waveguides initially contained: (a) uniform BECs, (b) two DS aligned at $x = 0$, (c) JV solution located at $x = 0$. The image (d) is the relative intensity between (b) and (c); $\nu = 0.01$, $t = 100$, $d = 2^{-3/2}$, $z_0 = 3$. The unit of x and y is the coherence length l_c .

the cloud of length L can be ignored. This imposes the limitation $\sqrt{t} \ll L$ in the chosen units. We also ignore quasi-1D thermal fluctuations. In other words, the phase-correlation length L_φ [12] is taken larger than the system size L . In reality this is too strong of a requirement — the discussed feature can be seen when $L_\varphi \geq L_s$.

Employing the ansatz (35,36), the density after time t (such that $R(t) \gg d$, that is, $t \gg d^2$) becomes

$$n(x, y, z) = \frac{e^{-\frac{(y^2+z^2)d^2}{t^2}}}{t^3} \left| \int dx_1 e^{-ix_1^2/2t} f(x_1) \left(\sin\left(\frac{zz_0}{t}\right) \cos\left(\frac{xx_1}{t}\right) \psi''(x_1) + i \cos\left(\frac{zz_0}{t}\right) \sin\left(\frac{xx_1}{t}\right) \psi'(x_1) \right) \right|^2 \quad (38)$$

where the overall factor is dropped, and $\psi'(x) = \sqrt{1+\nu} \tanh(sx)$ and $\psi''(x) = Q_0/\cosh(sx)$ are, respectively, the real and imaginary parts of the JV solution [5] given by $s = 2\sqrt{\nu}$, $Q_0 = \pm\sqrt{1-3\nu}$. The signs \pm are due to two possible directions of the current circulation in the JV. It is instructive to consider three distinctive cases: i) two uniform condensates, which can be reproduced from eq.(38) by setting $\psi' = 0$ and $\psi'' = 1$; ii) two identical DSs at $x = 0$, which can be obtained by setting $\psi'' = 0$; and iii) the JV. In the case i), taking the limit $L \rightarrow \infty$ and performing explicit integration, one finds

the well known parallel fringes $n(x, y, z) \sim \cos^2(zz_0/t)$. In the case ii), there is a zero at $x = 0$. Its width can be estimated from eq.(38) as $\delta x \approx \sqrt{t}$ in the limit $\sqrt{t} \gg 1/s$, that is, when the DS length $L_s = 1/s$ has expanded significantly: $L_s \ll t/L_s$. The actual density profile can be obtained analytically for $1/s \ll |x| \leq \sqrt{t}$ as

$$n_{DS}(x, y, z) = \frac{4(1+\nu)e^{-\frac{(y^2+z^2)d^2}{t^2}}}{t^3} x^2 \cos^2\left(\frac{zz_0}{t}\right). \quad (39)$$

It features the parallel fringes with the central zero as shown in Fig.3b.

The JV IP can easily be understood by analyzing the vicinity $x = 0$. Indeed, for $1/s \ll |x| \leq \sqrt{t}$, the $\tanh(sx)$ function can be replaced by a step function and $Q_0/\cosh(sx)$ effectively becomes $\delta(x) \int dx Q_0/\cosh(sx) = \pi Q_0 \delta(x)/s$. Thus, the density profile due to the JV becomes

$$n_{JV}(x, y, z) = \frac{e^{-\frac{(y^2+z^2)d^2}{t^2}}}{t^3} (2\sqrt{1+\nu} \cos\left(\frac{zz_0}{t}\right) x \pm \frac{\pi\sqrt{1-3\nu}}{2\sqrt{\nu}} \sin\left(\frac{zz_0}{t}\right))^2. \quad (40)$$

The profile of the zeros of the density $n = n(x, z, t)$ defines the feature specific for the JV. In the DS case, zeros belong to the set of mutually orthogonal lines $x = 0$ and $z = \pi(n+1/2)t/z_0$, with n integer. In the JV case, represented by eq.(40), the lines of zeros do not cross any more and obey the condition

$$x = \pm \frac{\pi}{4} \sqrt{\frac{1-3\nu}{\nu(1+\nu)}} \tan\left(\frac{sz}{t}\right) \quad (41)$$

The inclined tangential feature seen on Fig.3c is a consequence of the smooth relative phase change from 0 to 2π in the JV. It is also worth noting that the JV circulations in different directions produce tangential slope of different sign in the IP.

On Fig.(3) we have plotted column densities (integrated over y) at $t = 100$ ($t = 50ms$ in usual units, which is a typical experimental expansion time after which the absorption image is taken). It should be noted that the above presented IPs correspond to the case when the separation between the waveguides z_0 is significantly larger than the transverse extension d . Obviously, in this situation the tunneling ν is essentially zero. If one tries to decrease z_0/d , the visibility of the fringes worsens due to the exponential factor in (38) so that for $z_0/d \sim 1$ just one central fringe is seen. Thus, in order to achieve a good resolution, the clouds should be quickly separated from each other and, then, immediately released. Under these conditions, the JV solution formed at a closed proximity between the waveguides will have no time to be distorted by the inter-particle interactions after the tunneling is cut off. Obviously, the duration of the waveguides' separation from some distance $z_0 \approx d$ (when the tunneling is finite) to, e.g., $z_0 \approx 10d$ (when the tunneling

is, practically, zero) is limited from below by the inverse frequency $\approx d^2$ of the radial confinement. From above, it is limited by the axial response time $1/\mu \approx l_c^2$. This requirement can safely be satisfied if $(d/l_c)^2 \ll 1$, that is, in the quasi-1D regime.

The above discussion has been limited to destructive imaging of the JV. Very recently, a non-destructive method has been employed [13], [14] to continuously sample the relative phase of two spatially separated BECs. Tilted fringes in the interference pattern of the outcoupled matter waves have been seen as an evidence of axial gradients of the relative phase [14]. This method can also be very useful for detecting the Josephson vortex and its conversion into the dark soliton and vice versa. The out-coupling pulse produces recoil atoms characterized by the wavefunction which, in the co-moving frame, is a replica (apart from the numerical factor) of the wavefunction of the confined atoms. Thus, the interference pattern produced by the outcoupled clouds will be identical to the one discussed above.

V. CONCLUSION

The atomic Bose Josephson vortex can be created by the phase imprinting technique and detected due to its

particular feature in the column density by absorption imaging performed after some ballistic expansion. The Josephson vortex can be controllably displaced by imposing tunneling current (created by disbalance of chemical potentials) between the waveguides. In quasi-1D, motion of an atomic Josephson vortex is strongly coupled to the current circulation through the phase-slip effect. This leads to a destruction of the circulation for the vortex speeds above a certain value determined by the Josephson coupling. In contrast to the standard approach to Josephson vortices in superconductors within the Sine-Gordon formalism, a description of the coupling between the center of mass motion and the circulation necessarily involves both density and phase variations.

VI. ACKNOWLEDGEMENT

This work is supported by the NSF grant PHY-0426814 and by the PSC-CUNY grant 66556-0035.

-
- [1] S. Burger, K. Bongs, S. Dettmer, W. Ertmer, K. Sengstock, A. Sanpera, G. V. Shlyapnikov, M. Lewenstein, Phys. Rev. Lett. **83**, 5198 (1999); B.P. Anderson, P.C. Haljan, C.A. Regal, D.L. Feder, L.A. Collins, C. W. Clark, E. A. Cornell, *ibid.* **86**, 2926 (2001); J. Denschlag, J. Denschlag, J. E. Simsarian, D. L. Feder, C. W. Clark, L. A. Collins, J. Cubizolles, L. Deng, E. W. Hagley, K. Helmerson, W. P. Reinhardt, S. L. Rolston, B. I. Schneider, W. D. Phillips, Science **287**, 97 (2000).
 - [2] Kevin E. Strecker, Guthrie B. Partridge, Andrew G. Truscott and Randall G. Hulet, Nature (London) **417**, 150 (2002); L. Khaykovich, F. Schreck, G. Ferrari, T. Bourdel, J. Cubizolles, L. D. Carr, Y. Castin, C. Salomon, Science **296**, 1290 (2002).
 - [3] A. Fetter and A. Svidzinsky, J. Phys.: Condens. Matter **13**, R135 (2001).
 - [4] C. M. Savage and J. Ruostekoski, Phys. Rev. Lett. **91**, 010403 (2003).
 - [5] V. M. Kaurov and A. B. Kuklov, Phys. Rev. A **71**, 011601(R) (2005).
 - [6] Y. Shin, M. Saba, T.A. Pasquini, W. Ketterle, D.E. Pritchard, A.E. Leanhardt, Phys. Rev. Lett. **92**, 050405 (2004).
 - [7] Y. Shin, C. Sanner, G.-B. Jo, T. A. Pasquini, M. Saba, W. Ketterle, D. E. Pritchard, M. Vengalattore, M. Prentiss, Phys. Rev. A **72**, 021604(R) (2005).
 - [8] A. Barone, G. Paterno, *Physics and Applications of the Josephson Effect*, John Wiley & Sons, New York - Singapore, 1982.
 - [9] M.R. Andrews, C.G. Townsend, H.-J. Miesner, D.S. Durfee, D.M. Kurn, and W. Ketterle, Science **275**, 637-641 (1997).
 - [10] S. Inouye, S. Gupta, T. Rosenband, A. P. Chikkatur, A. Gorlitz, T. L. Gustavson, A. E. Leanhardt, D. E. Pritchard, and W. Ketterle, Phys. Rev. Lett. **87**, 080402 (2001); F. Chevy, K. W. Madison, V. Bretin, and J. Dalibard, Phys. Rev. A **64**, 031601(R) (2001);
 - [11] Eric L. Bolda and Dan F. Walls, Phys. Rev. Lett. **81**, 5477 (1998); J. Tempere and J. T. Devreese, Solid State Commun. **108**, 993 (1998).
 - [12] D.S. Petrov, G.V. Shlyapnikov, and J.T.M. Walraven, Phys. Rev. Lett. **85**, 3745 (2000); *ibid.* **87**, 050404 (2001); S. Dettmer, D. Hellweg, P. Ryytty, J. J. Arlt, W. Ertmer, K. Sengstock, D. S. Petrov, G. V. Shlyapnikov, H. Kreutzmann, L. Santos, M. Lewenstein, *ibid.* **87**, 160406 (2001).
 - [13] M. Saba, T. A. Pasquini, C. Sanner, Y. Shin, W. Ketterle, D. E. Pritchard, Science **307**, 1945 (2005).
 - [14] Y. Shin, G.-B. Jo, M. Saba, T. A. Pasquini, W. Ketterle, and D. E. Pritchard, Phys. Rev. Lett. **95**, 170402 (2005).